12778 *Biochemistry* **1996,** *35,* 12778−12787

# Characterization of the Metal Ion Binding Helix−Hairpin−Helix Motifs in Human DNA Polymerase $\beta$ by X-ray Structural Analysis[†,‡]

Huguette Pelletier*,[§] and Michael R. Sawaya[||]

*Department of Chemistry and Biochemistry, University of California, San Diego, La Jolla, California 92093-0506, and Verna and Marrs McLean Department of Biochemistry, Baylor College of Medicine, One Baylor Plaza, Houston, Texas 77030*

*Received April 2, 1996; Revised Manuscript Received June 18, 1996*[⊗]

ABSTRACT: X-ray crystallographic studies have shown that DNA binding by human polymerase $\beta$ (pol $\beta$) occurs primarily through two structurally and sequentially homologous helix−hairpin−helix (HhH) motifs, one in the fingers subdomain and the other in the 8-kDa domain [Pelletier, H., Sawaya, M. R., Wolfle, W., Wilson, S. H., & Kraut, J. (1996a) *Biochemistry 35*, 12742−12761]. In that DNA binding by each HhH motif is facilitated by a metal ion, we set out to determine the identity of the metal ion that most likely binds to the HhH motif in vivo. Crystal soaking experiments were performed on human pol $\beta$−DNA cocrystals with $Mg^{2+}$, $Ca^{2+}$, $Na^{+}$, and $K^{+}$, the four most prevalent metal ions in the cell, and in each case a data set was collected and the resulting structure was refined. Under the conditions tested, the HhH motifs of pol $\beta$ have an affinity for these biologically prevalent metal ions in the order $Mg^{2+} < Ca^{2+} < Na^{+} < K^{+}$, with $K^{+}$ displaying the strongest binding. Crystals soaked in the presence of $Tl^{+}$, a commonly used spectroscopic probe for $K^{+}$, were too X-ray-sensitive to establish the binding behavior of $Tl^{+}$, but soaking experiments with $Ba^{2+}$ and $Cs^{+}$ resulted in relatively stable crystals that gave evidence of metal ion binding in both HhH motifs, confirming that larger monovalent and divalent metal ions are capable of binding to the HhH metal sites. Although $Mn^{2+}$, which has been categorized as a potent polymerase mutagen, binds to the HhH motifs with a greater affinity than $Mg^{2+}$, $Mn^{2+}$ does not bind to the HhH motifs in the presence of equimolar concentrations of $Na^{+}$. These results suggest that in vivo, where $Mn^{2+}$ is present only in trace amounts, $Mn^{2+}$ probably does not have a large effect on DNA binding and may instead manifest a mutagenic effect on pol $\beta$ primarily by distorting nucleotide binding or by directly affecting the catalytic step [Pelletier, H., Sawaya, M. R., Wolfle, W., Wilson, S. H., & Kraut, J. (1996b) *Biochemistry 35*, 12762−12777]. Crystal soaking experiments with 31-kDa apoenzyme crystals show that, in the absence of DNA, the HhH motif in the fingers subdomain binds metal ions with either much lower occupancy or not at all, indicating that metal ion binding is dependent on the presence of the DNA substrate.

Metal ions such as $Cd^{2+}$, $Co^{2+}$, $Ni^{2+}$, $Cr^{3+}$, and $Mn^{2+}$ have been classified as mutagens, and potential carcinogens, because they cause polymerases to make errors during DNA replication in vitro (Sirover & Loeb, 1976; Snow & Xu, 1991; Snow et al., 1993). Although one explanation for these observations is that mutagenic metal ions might bind to DNA in a nonspecific manner and cause abnormal structural distortions during DNA replication, the recent discovery, by X-ray crystal structural analyses, of four distinct metal ion binding sites in mammalian DNA pol $\beta$ (Sawaya et al., 1994; Pelletier et al., 1994, 1996a,b) has offered specific examples of how a metal ion might manifest its mutagenic effect on a polymerase. One metal ion, which is most likely a $Mg^{2+}$ ion in vivo, coordinates oxygen atoms from highly conserved carboxylate groups in the active site of pol $\beta$ and has been termed the catalytic metal ion; a second metal ion, which is also thought to be a $Mg^{2+}$ ion in vivo, is observed in pol $\beta$'s active site only when accompanied by a nucleotide or pyrophosphate and accordingly has been termed the nucleotide-binding metal ion; and finally, two other metal ion binding sites, away from the active site, have recently been discovered in two structurally and sequentially homologous helix−hairpin−helix (HhH) DNA binding motifs−one in the fingers subdomain and one in the 8-kDa domain (Pelletier et al., 1996a). It appears that a given metal ion mutagen can therefore alter pol $\beta$'s function in at least three different ways: (i) by directly affecting catalysis, (ii) by distorting nucleotide binding, or (iii) by distorting DNA binding.

Crystal soaking experiments have proven to be useful for studying the relative effects that various metal ions have on catalysis and nucleotide binding (i and ii above) in the active site of pol $\beta$ (Pelletier et al., 1996b). A typical soaking experiment consists of the following steps: (i) equilibrating a pol $\beta$−DNA cocrystal in a standard artificial mother liquor, (ii) transferring the equilibrated crystal to a soaking solution that is prepared by adding small amounts of concentrated stock solutions of metal ions and nucleotides to the standard artificial mother liquor, (iii) allowing the crystal to soak in the metal ion−nucleotide solution for a set time, (iv) collecting X-ray diffraction data on the crystal, and (v)

---

[†] Supported by NIH Grant GM52860. This work was also supported in part by grants from the National Institutes of Health (NIH), the R. A. Welch Foundation, and a grant of computing time from the San Diego Super Computer Center.

[‡] Coordinates and reflection data are available from the Brookhaven Protein Data Bank and may also be obtained by sending an e-mail request to hug@bcm.tmc.edu.

[*] To whom correspondence should be addressed.

[§] Baylor College of Medicine.

[||] University of California, San Diego.

[⊗] Abstract published in *Advance ACS Abstracts*, September 1, 1996.

analyzing the resulting structure to see if any differences can be observed between the nucleotide-soaked and a non-nucleotide-soaked crystal. With this technique relatively small changes in the constitution of the soaking solution resulted in crystallographically observable differences in nucleotide binding and catalysis, allowing a structural basis for metal ion mutagenicity and nucleotide selectivity in pol $\beta$ to be presented (Pelletier et al., 1996b).

In an attempt to extend our knowledge of the metal ion binding behavior of pol $\beta$ to include protein−DNA interactions, the work presented here focuses on the DNA-binding HhH motifs in the fingers subdomain and the 8-kDa domain of pol $\beta$. Similar crystal soaking experiments as those described above have been carried out on pol $\beta$−DNA cocrystals with the exception that no nucleotides have been included in the soaking solutions (only various metal ions have been included), and a sodium-free artificial mother liquor was utilized to allow access to the metal ion binding site in the HhH motifs.[1] These experiments were performed to address such questions as the following: Do the DNA-binding HhH motifs in the fingers subdomain and the 8-kDa domain favor a specific metal ion? Do metal ions that are classified as polymerase mutagens distort DNA binding in the crystal structure? And finally, do metal ions bind to the HhH motifs in the absence of DNA?

Attempts were made to answer the first question by taking advantage of the fact that $Na^+$ and $Mg^{2+}$ possess relatively low numbers of electrons (only 10 electrons each) and are therefore difficult to detect crystallographically. Because of this, it was possible to carry out competitive binding experiments between relatively "invisible" metal ions ($Na^+$ and $Mg^{2+}$) and more easily detectable metal ions such as $K^+$ and $Ca^{2+}$, which have greater numbers of electrons. As an example, we observed strong electron density for a $Ca^{2+}$ ion in both HhH motifs when pol $\beta$−DNA cocrystals were soaked in $CaCl_2$ alone or in an equimolar $CaCl_2-MgCl_2$ mixture, but only very weak electron density was observed in the HhH metal ion sites when a pol $\beta$−DNA cocrystal was soaked in an equimolar $CaCl_2-NaCl$ mixture. These results suggest that whereas $Mg^{2+}$ did not displace $Ca^{2+}$ from the HhH metal sites, $Na^+$ did. With this technique a relative order of metal ion affinities for the HhH motifs emerged such that $Mg^{2+} < Ca^{2+} < Na^+ < K^+$, where $K^+$ displayed the strongest binding.

With regard to the second question, which addresses distortions in DNA binding, although the resolution of the crystal structures reported here (2.7−3.5 Å) precludes a definitive analysis, only the larger metal ions tested ($Cs^+$ and $Ba^{2+}$) showed some evidence of distorting DNA binding in the crystal structure. In that no obvious structural distortions were observed when $Mn^{2+}$ bound to the HhH metal sites, and in that $Na^+$ competes very well with $Mn^{2+}$ for binding in the HhH motif, it is suggested that a potent polymerase mutagen like $Mn^{2+}$ probably does not have a significant effect on DNA binding for pol $\beta$ in vivo.

Finally, in answer to the third question, none of the metal ions tested bound to HhH motif of the fingers subdomain when pol $\beta$ 31-kDa apoenzyme crystals (which lack the 8-kDa domain)[2] were soaked in various metal ion solutions, indicating that metal ion binding to the HhH motifs is dependent on the presence of the DNA substrate. In light of recent findings that the HhH motifs of pol $\beta$ are also present in at least two other DNA repair enzymes (Pelletier et al., 1996a); the metal ion binding behavior of the HhH motifs reported here may be applicable to many HhH-containing proteins.

## EXPERIMENTAL PROCEDURES

*Crystallizations*. The human DNA pol $\beta$−DNA cocrystals utilized in our soaking experiments have 7 base pairs of double-stranded DNA bound in the pol $\beta$ binding channel and are referred to as 7bp crystals (Pelletier et al., 1996a). Protein−DNA sample preparations and crystallizations for the 7bp crystals were performed as previously described (Pelletier et al., 1996a,b). In fact, many of the crystals utilized in the experiments reported here came from the same batch of crystals that had been grown for the previous crystal soaking experiments (Pelletier et al., 1996b). Despite being over a year old, these crystals showed no noticeable deterioration in diffraction quality. The crystals are orthorhombic and belong to space group $P2_12_12$ ($a = 179.0$, $b = 57.5$, $c = 48.5$ Å) with one pol $\beta$ molecule in an asymmetric unit. Crystals of recombinant 31-kDa pol $\beta$ were grown as previously described (Sawaya et al., 1994). These crystals are orthorhombic and belong to space group $P2_12_12$ ($a = 120.6$, $b = 63.5$, $c = 38.2$ Å) with one 31-kDa molecule per asymmetric unit.

*Crystal Soaks and Data Collection*. Crystal soaking experiments were carried out as previously described (Pelletier et al., 1996b) with the exception that a sodium-free artificial mother liquor (16% PEG 3350 and 100 mM imidazole, pH 6.5) was utilized for the experiments reported here. Metal ion soaking solutions were made by starting with 1 mL of artificial mother liquor and then adding microliter quantities of concentrated stock solutions (in deionized and distilled $H_2O$) of various metal ions, resulting in the final concentrations listed under soaking conditions (Table 1).[3] Unless otherwise noted in Table 1, crystals were soaked in the designated soaking solutions for 24−26 h before data collection, and data collection typically lasted about 25 h. X-ray diffraction data were collected on a multiwire area detector (Hamlin et al., 1995) (San Diego Multiwire Systems) with monochromatized CuKα radiation (Rigaku RU200 rotating-anode X-ray generator), and intensity observations for each data set were processed with a local UCSD Data Collection Facility software package (Howard et al., 1985).

*Structure Determinations and Refinements*. Previously determined and refined human pol $\beta$−DNA and rat 31-kDa

---

[1] A seemingly odd result that we noted in passing during the previous soaking experiments was that, despite the relatively high concentrations of the metal ions utilized (up to 5 mM), we never observed strong metal ion binding in the HhH motifs of pol $\beta$ (Pelletier et al., 1996b). The results reported here offer an explanation for this observation—we have discovered that $Na^+$ ions, which are difficult to detect crystallographically, bind to the HhH motifs of pol $\beta$ relatively strongly, and because all previous crystal soaking experiments had been carried out in the presence of 150 mM NaCl and/or 100 mM Na-MES buffer, tightly bound $Na^+$ ions most likely blocked the binding of other metal ions in the HhH metal sites.

[2] Although the 31-kDa protein lacks the N-terminal 8-kDa domain and hence, one of the two HhH motifs of pol $\beta$, we nevertheless utilized 31-kDa apoenzyme crystals for the metal ion soaking experiments reported here because the 31-kDa crystals diffract to much higher resolutions than apoenzyme crystals of the full protein (Sawaya et al., 1994). We are assuming that, in the absence of DNA, the metal ion binding behavior of the HhH motif in the 8-kDa domain is similar to that of the HhH motif in the fingers subdomain.

Table 1: Data Collection and Refinement Statistics

| soaking conditions[a] | PDB code | $d_{min}$ (Å) | $\langle I/\sigma\rangle$[b] | completeness[c] (%) | $R_{sym}$[d] (%) | difference density?[e] | Final $R$[f] (%) | Metal $B$-factor[g] (Å$^2$) | |
|---|---|---|---|---|---|---|---|---|---|
| | | | | | | | | fingers | 8-kDa |
| native, natural mother liquor | 9ICJ | 3.1 | 1.8 | 88 | 5.6 | NA/NA | 14.9 | 3[h] | 75[h] |
| native, artificial mother liquor, pH 6.5 | 1ZQG | 3.1 | 1.8 | 89 | 7.0 | NA/NA | 16.2 | 10[h] | 51[h] |
| native, artificial mother liquor, pH 7.5[i] | 1ZQH | 3.1 | 1.8 | 90 | 6.2 | NA/NA | 22.9 | 1[h] | 3[h] |
| 150 mM $CaCl_2$ | 1ZQD | 3.5 | 1.9 | 73 | 7.8 | yes/yes | 14.4 | 14 | 66 |
| 15 mM $CaCl_2$ (6 h) | 1ZQC | 3.2 | 1.8 | 89 | 6.8 | yes/yes | 17.3 | 23 | 93 |
| 15 mM NaCl, 15 mM $CaCl_2$ (12 h) | 1ZQO | 3.2 | 1.8 | 90 | 7.2 | no/no | 15.9 | 13 | 32 |
| 15 mM $CaCl_2$, 15 mM $MgCl_2$ (12 h) | 1ZQJ | 3.3 | 1.9 | 74 | 7.4 | yes/yes | 20.6 | 19 | 42 |
| 150 mM KCl | 1ZQI | 2.7 | 1.8 | 89 | 5.5 | yes/yes | 17.9 | 16 | 65 |
| 150 mM KCl, pH 7.5 (3 days)[i] | 1ZQA | 2.7 | 1.8 | 87 | 5.7 | yes/yes | 17.9 | 15 | 60 |
| 75 mM KCl, 75 mM NaCl | 1ZQP | 2.8 | 1.9 | 83 | 5.5 | yes/yes | 16.6 | 31 | 61 |
| 75 mM KCl, 75 mM $MgCl_2$ | 1ZQK | 3.2 | 1.8 | 88 | 7.0 | yes/yes | 14.5 | 21 | 81 |
| 150 mM CsCl (3 days) | 1ZQF | 2.9 | 1.8 | 90 | 8.2 | yes/yes | 18.3 | 42 | 59 |
| 150 mM $BaCl_2$ (2 days) | 1ZQB | 3.2 | 1.9 | 74 | 7.8 | yes/yes | 14.6 | 28 | 61 |
| 15 mM $BaCl_2$, 15 mM NaCl (3 days) | 1ZQN | 3.0 | 1.8 | 89 | 7.6 | yes/yes | 17.7 | 53 | 56 |
| 15 mM $MnCl_2$ (36 h) | 1ZQM | 3.2 | 1.8 | 70 | 7.2 | yes/yes | 14.9 | 26 | 99 |
| 15 mM NaCl, 15 mM $MnCl_2$ | 1ZQQ | 3.3 | 1.8 | 75 | 6.7 | no/no | 16.3 | 4 | 23 |
| 15 mM $MnCl_2$, 15 mM $MgCl_2$ (12 h) | 1ZQL | 3.3 | 1.9 | 88 | 8.3 | yes/yes | 15.9 | 68 | 100 |
| saturated $CrCl_3$ (2 days) | 1ZQE | 3.7 | 2.0 | 74 | 8.2 | yes/no | 17.1 | 30 | [j] |
| 15 mM $NiCl_2$ (12 h) | 1ZQR | 3.7 | 1.8 | 70 | 9.3 | no/no | 17.3 | 61[h] | [j] |
| 0.5 mM TlCl (1 h) | 1ZQS | 3.3 | 1.8 | 73 | 8.5 | no/no | 16.5 | 1[h,k] | 19[h,k] |
| 31-kDa, artificial mother liquor | 1ZQU | 2.6 | 1.9 | 96 | 7.3 | NA/NA | 19.8 | 53[l] | NA |
| 31-kDa, 150 mM $CaCl_2$ | 1ZQV | 2.7 | 2.7 | 83 | 5.3 | no/NA | 24.9 | 36[l] | NA |
| 31-kDa, 150 mM CsCl | 1ZQW | 2.3 | 1.9 | 95 | 7.5 | no/NA | 19.7 | 33[l] | NA |
| 31-kDa, 150 mM KCl[m] | 1ZQX | 2.5 | 2.1 | 92 | 7.4 | no/NA | 22.6 | 53[l] | NA |
| 31-kDa, 50 mM $MgCl_2$[m] | 1ZQY | 2.3 | 2.0 | 92 | 6.6 | no/NA | 19.8 | 68[l] | NA |
| 31-kDa, 50 mM $MnCl_2$[m] | 1ZQZ | 2.7 | 2.1 | 95 | 7.9 | no/NA | 20.2 | 75[l] | NA |
| 31-kDa, 5 mM $MnCl_2$ (1 month)[n] | 1NOM | 3.0 | 1.9 | 97 | 6.4 | no/NA | 18.4 | 52[l] | NA |

[a] See Experimental Procedures for a description of how soaking solutions were prepared and how soaking experiments were carried out. Unless otherwise indicated in parentheses, crystals were soaked for 1 day before data collection began. With the exception of the last six data sets, which were obtained from rat pol $\beta$ 31-kDa crystals that were grown as described (Sawaya et al., 1994), all data sets were obtained from human pol $\beta-$DNA cocrystals in which the DNA is 7 base pairs long [termed 7bp (Pelletier et al., 1996a)]. [b] Average ratio of observed intensity to background in the highest resolution shell of reflections. [c] Incomplete data sets (less than 85%) were the result of X-ray-sensitive crystals that slowly died in the X-ray beam before a complete data set could be collected. [d] $R_{sym} = \sum|I_{obs} - I_{avg}|/\sum I_{avg}$. [e] A yes in this column indicates that clear electron density ($>5\sigma$) was observed in the HhH metal ion site in $F_{o(metal)} - F_{o(native)}$, $\alpha_{c(native)}$ difference Fourier maps, where $F_{o(native)}$ represents data from the native crystal soaked in artificial mother liquor. A yes or a no answer for each HhH metal site (for the fingers subdomain and the 8-kDa domain, respectively) are given and are separated by a slant. NA means not applicable. [f] Final $R = \sum|F_{obs} - F_{calc}|/\sum F_{obs}$, including all data between 20 Å and the maximum resolution. As a part of the TNT program package (Tronrud et al., 1987), a scaling function was applied during refinements to compensate for a lack of solvent continuum in the model for the low-order reflections (Moews & Kretsinger, 1975). [g] In cases where two different metal ions were present in the same soaking solution, the scattering factors for the first metal ion listed under soaking conditions were utilized during refinement and their resulting $B$-factors are the ones listed. [h] Water molecules could have been modeled into electron density at the HhH metal sites for these structures, but we chose to model $Na^+$ ions in the metal sites instead because of geometry considerations, as described in the text (Figure 1). [i] The artificial mother liquor differed slightly for these crystals such that imidazole, pH 7.5, was utilized as the buffer instead of imidazole, pH 6.5. [j] No electron density was observed in these metal sites, which may be an artifact of the poor resolution of the data. [k] Although no difference density was observed for the $Tl^+$ ion, the low $Na^+$ $B$-factors that resulted after refinement give some indication that $Tl^+$ ions may have bound at a very low occupancy (see footnote 3). [l] This $B$-factor is given for a water molecule that occupies the metal ion binding site in the absence of DNA (Figure 1, bottom). [m] The artificial mother liquor differed slightly for these crystals such that 100 mM Tris, pH 7.5 (sodium-free), was utilized as the buffer instead of 100 mM imidazole, pH 6.5. [n] The artificial mother liquor for this crystal consisted of 15% PEG 1500, 50 mM NaCl, 75 mM Hepes, pH 7.5, and 0.1 mM DTT and was meant to mimic the $Mn^{2+}$-soaking conditions reported by another group (Davies et al., 1994). Results of the $Mn^{2+}$-soaked 31-kDa crystal reported by Davies et al. differ from our results in that we only observe one $Mn^{2+}$ bound in the pol $\beta$ active site (Pelletier et al., 1994, 1996; Sawaya et al., 1994; Pelletier, 1994), whereas they report seeing two $Mn^{2+}$ ions bound in the pol $\beta$ active site (Davies et al., 1994). The data for the Mn-soaked crystal structure reported by Davies et al. have not been made available.

apoenzyme crystal structures (Pelletier et al., 1996a; Sawaya et al., 1994) were utilized as starting structures for the "artificial mother liquor" data sets reported in Table 1. The data set for the pol $\beta-$DNA cocrystal listed in Table 1 as "native, natural mother liquor" is the same data set listed in previous tables (Pelletier et al., 1996a,b). Difference Fourier maps [$F_{o(metal)} - F_{o(native)}$, $\alpha_{c(native)}$] for the metal-soaked crystals were calculated with $F_{o(native)}$ representing data from the artificial mother liquor-soaked crystal (Table 1). Subsequent refinement steps were carried out with the TNT program package (Tronrud et al., 1987). All structures listed in Table 1 have good geometry, with root-mean-square (rms) deviations in bond lengths and bond angles less than or equal to 0.020 Å and 3.0°, respectively.

## RESULTS AND DISCUSSION

*$Na^+$ Ion Binding.* Before metal ion soaking experiments were carried out, an attempt was made to remove bound $Na^+$ ions from the HhH motifs of pol $\beta$ by soaking a native pol $\beta-$DNA crystal in artificial mother liquor alone, with no $Na^+$ ions present (Table 1). The resulting structure still had observable electron density in the metal sites of both HhH motifs, and the density was interpreted to be either water

---

[3] Although little evidence of metal ion binding was observed for $Tl^+$-soaked crystals (Table 1), this may be because we had to use such low concentrations of the metal ion (0.5 mM) before a complete data set could be collected. Higher TlCl concentrations resulted in cracked crystals that either did not diffract at all or were too sensitive to X-rays for a complete data set to be collected. A great effort went into trying to determine the binding behavior of $Tl^+$ because it is a useful spectroscopic probe for $K^+$ (Douglas et al., 1990).

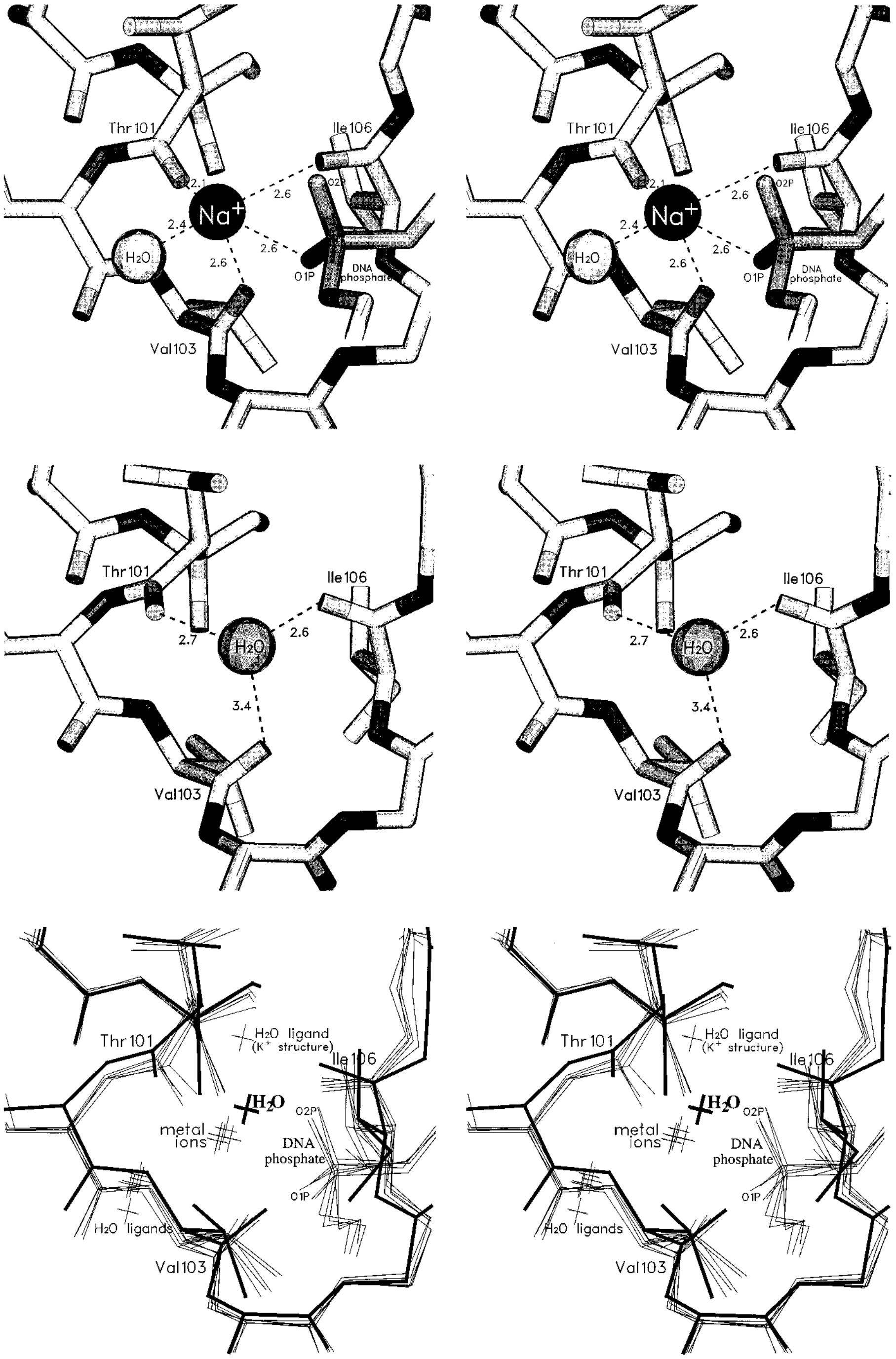

FIGURE 1: SETOR stereo diagrams (Evans, 1993) depicting differences in geometries for metal ion versus $H_2O$ binding in the HhH metal sites of pol $\beta$. Although $Na^+$ ions and water molecules are different to distinguish crystallographically, comparisons of the geometries observed in (top) $Na^+$ binding in the human DNA−pol $\beta$ complex crystal, versus (middle) $H_2O$-binding in the 31-kDa apoenzyme crystal, show that the identity of the entity bound in the HhH metal site may be determined by geometry considerations alone. As shown by the superposed structures in the bottom panel, the geometry of the $Na^+$ ion in the top panel, which includes short coordinate bond distances and a water ligand, was observed for all other metal ions tested (lighter shade) ($Ba^{2+}$, $Ca^{2+}$, $Cr^{3+}$, $Cs^+$, $K^+$, and $Mn^{2+}$) (Table 1). The position of the water molecule in the 31-kDa apoenzyme crystal structure (darker shade) did not vary significantly among any of the 31-kDa structures reported in Table 1, including those soaked in metal ion solutions. The lone water molecule toward the top of the metal site represents the sixth ligand of a bound $K^+$ ion from the $K^+$-soaked crystal structure (Table 1). All bond distances are in angstroms.

molecules or tightly bound $Na^+$ ions that had remained in the metal sites despite the back-soaking efforts. As was previously argued on the basis of geometry considerations (Pelletier et al., 1996a), the short bond distances between the entities that are bound in the HhH metal sites and the protein carbonyl oxygen atoms indicate that the HhH metal sites for this structure are most likely occupied by tightly bound $Na^+$ ions, and not water molecules (Figure 1, top). Similar electron density corresponding to either a water molecule or a $Na^+$ ion was observed in the HhH metal site of 31-kDa crystals soaked in artificial mother liquor alone, but in this case, the electron density was attributed to a water molecule because of the longer bond distances observed in this structure (Table 1; Figure 1, middle). These results indicate that the presence of only one additional oxygen ligand donated from the DNA phosphate group is enough to ensure strong metal ion binding in the HhH motifs—a conclusion that has been confirmed by soaking experiments

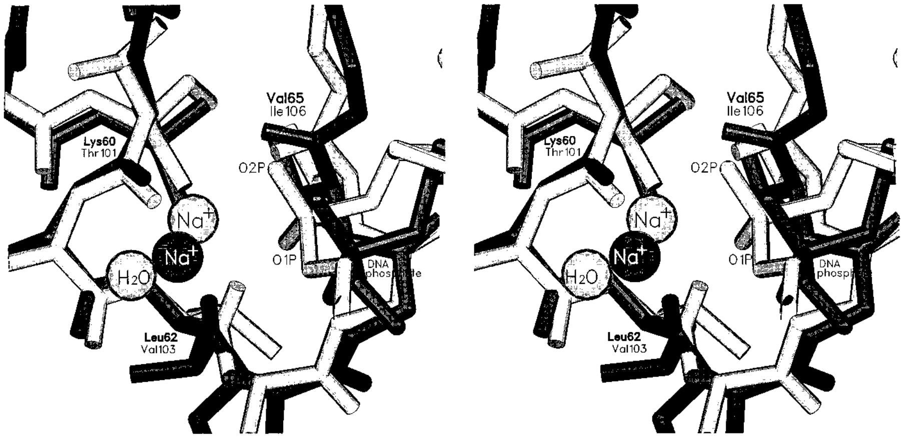

FIGURE 2: Comparison of the HhH metal ion sites in the fingers subdomain and 8-kDa domain. Superposition of the HhH metal sites of the fingers subdomain (lighter shade) versus the 8-kDa domain (darker shade) reveals that the 8-kDa domain binding site is slightly larger, possibly due to crystal packing distortions. The average *B*-factor for backbone atoms from lysine 60 to valine 65 of the 8-kDa domain is 30 Å$^2$, and the average *B*-factor for corresponding backbone atoms from threonine 101 to isoleucine 106 of the fingers subdomain is 15 Å$^2$. In that these average *B*-factors do not vary significantly from one structure to the next, the relatively large metal ion *B*-factors for the HhH motif of the 8-kDa domain, when compared with metal ion *B*-factors for the HhH motif of the fingers subdomain (Table 1), can safely be attributed to weaker binding of the metal ion in the 8-kDa domain. This stereo diagram was prepared with SETOR (Evans, 1993).

with other metal ions, as described below (Figure 1, bottom). Although it now appears that all of the pol $\beta$−DNA cocrystals utilized for the metal ion soaking experiments reported here probably had some residual $Na^+$ ions still bound to their HhH motifs, we have nevertheless demonstrated that, at relatively high concentrations, other metal ions are able to displace the bound $Na^+$ ions and bind in the HhH metal sites (Table 1). There is therefore no indication that residual $Na^+$ ions had any significant effect on the outcome of our results.

As was observed for all but the largest metal ions, metal ions consistently bound less tightly to the HhH metal site in the 8-kDa doamin than they did to the metal site in the fingers subdomain (Table 1). This can be explained by comparing the metal sites of the two HhH motifs, where it is evident that the metal ion binding pocket in the 8-kDa domain is slightly larger (Figure 2). Although this may represent a real difference in metal ion binding geometries for the two HhH motifs, it should be kept in mind that the protein−DNA interactions observed in the 8-kDa domain derive from intermolecular crystal packing contacts (Pelletier et al., 1996a), and therefore the geometry of the metal site in the 8-kDa domain may be slightly distorted. All subsequent metal sites depicted in the figures are from the HhH motif of the fingers subdomain.

*Metal Ion Selectivity of the HhH Motifs.* In the presence of DNA, the hairpin region of the HhH motifs in pol $\beta$ form small pockets that resemble one of the two $Ca^{2+}$ binding sites in phospholipase $A_2$ (Figure 3, top) (White et al., 1990), with the only significant difference being that, in phospholipase $A_2$, negatively charged oxygen ligands are donated from a carboxylate group rather than from a phosphate group. It is therefore not too surprising that a $CaCl_2$-soaked pol $\beta$−DNA cocrystal revealed strong electron density corresponding to bound $Ca^{2+}$ ions in both HhH metal sites (Table 1; Figure 3, bottom). However, unlike the $Ca^{2+}$ binding site in phospholipase $A_2$, the HhH metal sites of pol $\beta$ do not appear to be quite as selective for $Ca^{2+}$ binding only. With the exception of $Ni^{2+}$, which was one of the smallest metal ions tested, all other metal ions ($Ba^{2+}$, $Ca^{2+}$, $Cr^{3+}$, $Cs^+$, $K^+$, and $Mn^{2+}$) showed some evidence of binding to the HhH motifs, regardless of metal ion charge (Table 1; Figure 1, bottom). Although the result from the $Ni^{2+}$-soaked crystal gave some early indication that the HhH metal site may be selective for metal ion size, it nevertheless became apparent after the initial soaking experiments that if the HhH motifs of pol $\beta$ preferred to bind a specific metal ion, the mode of selectivity was relatively subtle.

Unlike the metal ions involved in catalysis and nucleotide binding for pol $\beta$, which are thought to be $Mg^{2+}$ ions in vivo (Kornberg & Baker, 1992), it was not clear, even after numerous crystal soaking experiments had been carried out in the presence of $Mn^{2+}$ (a good substitute for $Mg^{2+}$), that $Mg^{2+}$ ions were utilized by the HhH motifs of pol $\beta$ to facilitate DNA binding as well as catalysis (Pelletier et al., 1996b). It therefore became critical to establish the identity of the metal ion that might bind to the HhH metal sites under normal conditions in vivo, particularly if the mutagenic, and potentially carcinogenic, effects of "nonnormal" metal ions were to be studied. In our attempts to elucidate the subtleties of metal ion selectivity for the HhH motifs, we purposely narrowed our study, at least at first, to the four most prevalent metal ions in the cell—$Ca^{2+}$, $Mg^{2+}$, $Na^+$, and $K^+$, which are listed here in order of increasing availability.[4]

As discussed above, $Mg^{2+}$ and $Na^+$ are difficult to detect crystallographically because they each possess a relatively small number of electrons, but this characteristic was turned to our advantage in competitive-binding experiments. In a typical competitive-binding experiment, a pol $\beta$−DNA cocrystal was soaked in the presence of two different metal ions—one that is only weakly visible crystallographically ($Na^+$ or $Mg^{2+}$) and one that is easily detectable ($Ca^{2+}$ or $K^+$). With this technique, the identity of the metal ion bound in the HhH motifs could be established, depending on whether or not significant electron density was observed in the HhH metal sites of the soaked crystals. Perhaps the best example is provided by competitive-binding experiments with $CaCl_2$. Strong electron density was observed in the

---

[4] Due to difficulties in obtaining accurate measurements, in vivo metal ion concentrations are only tentatively known, particularly within the cell. However, the current opinion is that $Ca^{2+}$, $Mg^{2+}$, $Na^+$, and $K^+$ are present in the cell in approximate concentrations of 1 $\mu$M, 1 mM, 10 mM, and 100 mM, respectively (da Silva & Williams, 1991; Heaton, 1993; Cowan, 1993).

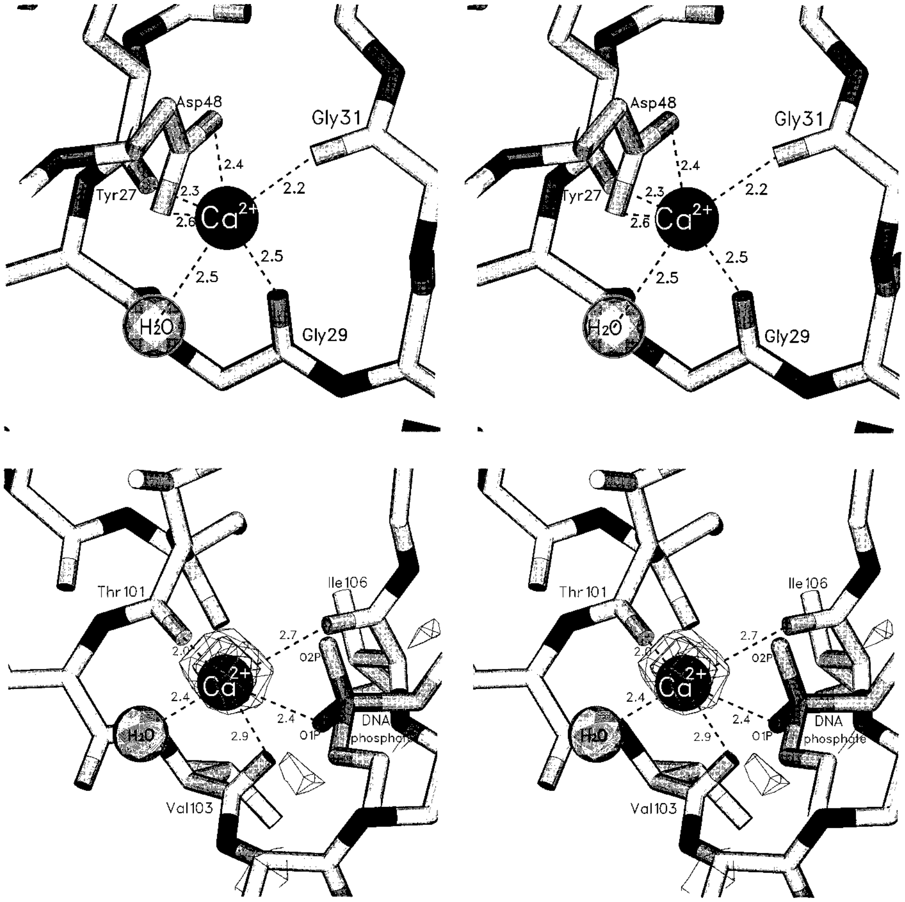

FIGURE 3: Comparison of the metal-binding sites of phospholipase $A_2$ and the HhH motif of pol $\beta$. (Top) Geometry of the bound $Ca^{2+}$ in the structure of phospholipase $A_2$, according to PDB coordinate file 1POA (White et al., 1990) versus (bottom) geometry of the bound $Ca^{2+}$ from the refined structure of the $Ca^{2+}$-soaked pol $\beta$−DNA cocrystal (PDB code 1ZQD) (Table 1). Electron density from the $F_{o(Ca)} - F_{o(native)}$, $\alpha_{c(native)}$ difference Fourier map is superposed on the structure in the bottom panel and is contoured at $5\sigma$. These stereo diagrams were prepared with SETOR (Evans, 1993).

HhH metal sites of a pol $\beta$−DNA cocrystal that was soaked in the presence of an equimolar mixture of $CaCl_2$ and $MgCl_2$, indicating that $Mg^{2+}$ did not displace bound $Ca^{2+}$ to any significant extent in the crystal structure. In contrast, there was no electron density visible in either HhH metal site when a pol $\beta$−DNA cocrystal was soaked in an equimolar mixture of $CaCl_2$ and NaCl, indicating that, unlike $Mg^{2+}$, $Na^+$ easily displaces (or completely blocks) $Ca^{2+}$ from the HhH metal sites in the crystal structure. These results not only help to establish an order of metal ion binding preference for the HhH metal sites (where $Mg^{2+} < Ca^{2+} < Na^+$), but results from the NaCl-soaked crystal, in particular, also supplied independent evidence that $Na^+$ ions do, indeed, bind to the HhH motifs [previous evidence for $Na^+$ binding was somewhat indirect in that it was based on geometry considerations alone (Figure 1, top) (Pelletier et al., 1996a)].

Similar competitive-binding experiments with KCl showed that neither $Mg^{2+}$ ions nor $Na^+$ ions were capable of displacing tightly bound $K^+$ ions from the HhH metal sites, at least not to any significant extent (Table 1). These results suggest that the HhH motifs have the highest affinity for $K^+$ so that, with regard to the most prevalent metal ions in the cell, the final order of HhH metal ion binding preference appears to be $Mg^{2+} < Ca^{2+} < Na^+ < K^+$. In that $K^+$, with an intracellular concentration of about 100 mM, is also the most prevalent metal ion in the cell (da Silva & Williams, 1991), $K^+$ is most likely the metal ion utilized by the HhH motifs of pol $\beta$ to facilitate DNA binding in vivo.

An interesting observation for the bound $K^+$ ions in the crystal structure is that, in contrast to the pentacoordinated square pyramidal geometry observed with $Na^+$ and $Ca^{2+}$ [Figures 1 (top) and 3 (bottom)], the $K^+$ ions in both HhH motifs display hexacoordinated octahedral geometry, with two oxygen ligands from the same DNA phosphate group participating in positioning the $K^+$ ion. The $K^+$ ion directly coordinates one phosphate oxygen while coordination to the second phosphate oxygen atom is mediated by a water molecule, forming an outer-sphere coordinate bond (Figure 4, top). Although the appearance of the second water molecule (the sixth ligand) in the $K^+$ structure could be the result of higher resolution data for the KCl-soaked crystal (Table 1),[5] this water molecule was not observed in the $Cs^+$ crystal structure, which was only slightly lower in resolution (Figure 4B). The apparently more stable coordination geometry observed for the $K^+$ ion is in agreement with results that $K^+$ ions bind to the HhH motifs relatively strongly and are most likely the metal ions utilized for DNA binding by the HhH motifs of pol $\beta$ in vivo.

*Size and Valency Considerations in Metal Ion Binding Affinities.* In that $Na^+$ and $Ca^{2+}$ have comparable ionic radii (0.97 and 0.99 Å for $Na^+$ and $Ca^{2+}$, respectively), results from the $CaCl_2$−NaCl soaking experiment suggest that the

---

[5] With the exception of $Tl^+$, it was common for crystals soaked in the presence of monovalent metal ions ($Na^+$, $K^+$, or $Cs^+$) to diffract better and display greater stability than crystals soaked in the presence of divalent or trivalent metal ions.

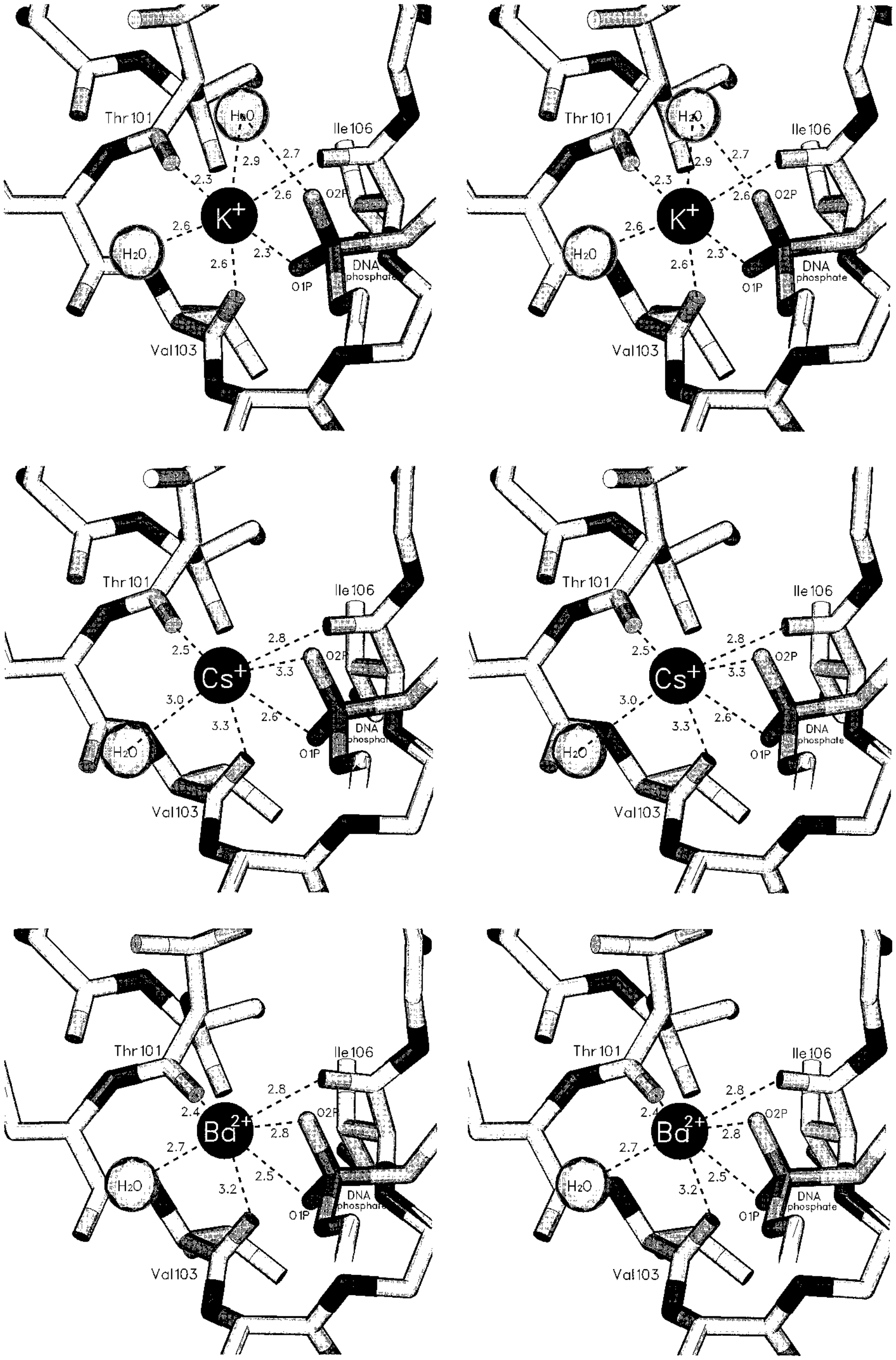

FIGURE 4: SETOR stereo diagrams (Evans, 1993) depicting results from $K^+$-soaked, $Cs^+$-soaked, and $Ba^{2+}$-soaked crystals. (Top) $K^+$ binding in the HhH metal site, showing clear octahedral geometry. $K^+$ is the only metal ion, of those tested, that displayed this geometry, as can be seen in Figure 1 (bottom). (Middle) $Cs^+$ binding, showing similar geometry as seen with $Na^+$ (Figure 1, top) and $Ca^{2+}$ (Figure 3, bottom), except that the coordinate bond distances are slighter longer. (C) $Ba^{2+}$ binding, showing strong coordination with both phosphate oxygens of the DNA phosphate. $Ba^{2+}$ was the only metal ion, of those tested, that directly coordinated both phosphate oxygens in this manner.

valency of the metal ion is an important selectivity factor for binding to the HhH motifs of pol $\beta$, with a monovalent metal ion being preferred over a divalent metal ion of similar size (Table 1). Then again, results from the KCl−NaCl soaking experiment, where the larger $K^+$ ion (ionic radius = 1.33 Å) displayed tighter binding than the smaller $Na^+$ ion, suggest that size also plays an important role in selectivity for the HhH metal sites. In order to investigate the relative contributions of size and valency in determining metal ion selectivity in the HhH motifs, we soaked a pol $\beta$−DNA cocrystal in equimolar concentrations of NaCl and $BaCl_2$ to see if $Na^+$, which has the preferred valency but incorrect size, could compete with $Ba^{2+}$, which has the preferred size (1.35 Å) but incorrect valency. Results show that $Na^+$ was not able to compete strongly with $Ba^{2+}$ for binding in the HhH motifs (Table 1; Figure 4, bottom), indicating that the size of the metal ion is more important than its charge for binding in the HhH metal site. The order of metal ion preference for the HhH metal sites, with $Ba^{2+}$ included, is therefore $Mg^{2+} < Ca^{2+} < Na^+ < Ba^{2+}, K^+$, making it even more apparent that the larger, more polarizable metal ions are favored by the HhH metal sites.

Although the order of metal ion preference outlined above suggests that the larger metal ions bind more tightly in the

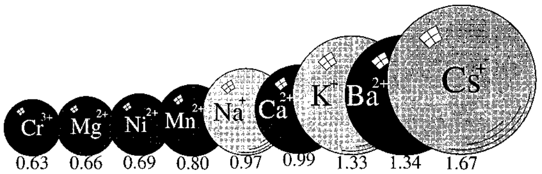

FIGURE 5: Relative sizes of the metal ions utilized in our crystal soaking experiments, in order of increasing ionic radii. Divalent and trivalent metal ions are depicted in darker shades. Ionic radii, in angstroms, were obtained from the CRC Handbook of Chemistry and Physics (Lide, 1992). This illustration was prepared with MOLSCRIPT (Kraulis, 1991).

HhH metal site, there must be a limit to the size of the metal ion that the HhH metal site can accommodate. Some evidence for this is provided by metal ion soaking experiments with $Cs^+$, which is the largest metal ion that we tested (ionic radius = 1.7 Å) (Figure 5). Unlike $K^+$ and $Ba^{2+}$, which appear to have very stable binding geometries in the HhH metal site (Figure 4, top and bottom panels), the coordination geometry for $Cs^+$ is similar to that observed for a smaller metal ion like $Ca^{2+}$, with the exception that the bond distances are slightly longer [compare Figure 4 (middle) with Figure 3 (bottom)]. Therefore, in much the same way that $Na^+$ may be just a little too small to compete well with $K^+$ and $Ba^{2+}$ for the HhH metal site, our results suggest that $Cs^+$ may be just a little too big. With this line of reasoning it is inferred that the HhH motifs may have similar binding affinities for $Na^+$ and $Cs^+$.

*Comparisons with the $Ca^{2+}$-Specific Binding Site in Phospholipase $A_2$.* With a little more now known about the metal ion selectivity patterns for the HhH motifs of pol $\beta$, it may be possible to determine why the metal ion binding pocket of the HhH motif prefers $K^+$, while a seemingly very similar metal ion binding pocket in phospholipase $A_2$ prefers $Ca^{2+}$ (Figure 3) (White et al., 1990). One reason for the difference in selectivity might be due to the fact that the metal ion in the HhH metal site coordinates oxygen atoms from a DNA phosphate group, whereas in phospholipase $A_2$, analogous oxygens are provided by a protein carboxylate group. However, closer inspection of the binding geometries in the two metal sites reveals a less obvious structural difference that may contribute significantly to metal ion selectivity. The best geometry for coordination to a carbonyl oxygen occurs when the metal−oxygen bond is coplanar with the trigonal carbonyl bound and is skewed at an angle of 120°. This is the case more nearly so with the three carbonyl oxygen ligands of the $Ca^{2+}$ ion in the phospholipase $A_2$ structure than with the carbonyl oxygen ligands of the metal ions in the HhH metal site (Table 2). In fact, the coordination geometry of the $K^+$ ion in the HhH metal site is much like that observed in many $K^+$-binding antibiotics such as valinomycin, enniatin B, nonactin, and monesin, where a centrally located $K^+$ ion in each structure forms numerous noncoplanar coordinate bonds to carbonyl oxygen atoms (Gale et al., 1981). These observations suggest that a larger, more polarizable metal ion such as $K^+$ may be better suited for the unfavorable carbonyl coordination geometry of the HhH metal site, whereas a smaller, "harder" metal ion like $Ca^{2+}$ may be better suited for the relatively more rigid carbonyl coordination geometry of the phospholipase $A_2$ metal site. A similar suggestion has already been made concerning the contribution of carbonyl oxygen geometry to selectivity in the $Ca^{2+}$ site of phospholipase $A_2$ (White et al., 1990), except in that case, the focus was on substrate specificity and not metal ion binding specificity.

Table 2: Geometries of Carbonyl Oxygen Ligands in the Phospholipase $A_2$ and Pol $\beta$ Metal Sites

| carbonyl oxygen−metal ion bond[a] | deviation from plane of carbonyl group (Å) | angle between C=O bond and O−metal ion bond |
|---|---|---|
| $C{=}O^{27}{-}Ca^{2+}$ | 0.5 | 161° |
| $C{=}O^{29}{-}Ca^{2+}$ | 0.9 | 167° |
| $C{=}O^{31}{-}Ca^{2+}$ | 0.4 | 157° |
| $C{=}O^{101}{-}K^{+}$ | 0.6 | 168° |
| $C{=}O^{103}{-}K^{+}$ | 1.3 | 177° |
| $C{=}O^{106}{-}K^{+}$ | 0.8 | 154° |
| $C{=}O^{101}{-}Ca^{2+}$ | 0.2 | 179° |
| $C{=}O^{103}{-}Ca^{2+}$ | 2.6 | 169° |
| $C{=}O^{106}{-}Ca^{2+}$ | 0.1 | 157° |

[a] Oxygen ligands from the backbone carbonyls of residues tyrosine 27, glycine 29, and glycine 31 of the $Ca^{2+}$ binding site in phospholipase $A_2$ are designated with the superscripts 27, 29, and 31, respectively. Oxygen ligands from the backbone carbonyls of residues threonine 101, valine 103, and isoleucine 106 of the HhH metal site in the fingers subdomain of pol $\beta$ are designated with the superscripts 101, 103, and 106, respectively. Data were taken from coordinate files (1POA) of phospholipase $A_2$ (Figure 3, top) (White et al., 1990), and the coordinate files (1ZQI and 1ZQC) of the $K^+$-soaked and $Ca^{2+}$-soaked crystal structures reported here (Table 1) [Figures 3 (bottom) and 4 (top)].

*Effects of Metal Ion Mutagens on DNA Binding.* The purpose of much of our previous crystal soaking experiments was to study the relative effects that various metal ion mutagens such as $Mn^{2+}$ and $Ni^{2+}$ have on nucleotide binding and catalysis in the active site of pol $\beta$ (Pelletier et al., 1996b). In an attempt to extend these studies to include the metal ion binding HhH motifs of pol $\beta$, competitive binding experiments similar to those described above for $Ca^{2+}$, $K^+$, and $Ba^{2+}$ were carried out with $Mn^{2+}$. Results from crystal soaking experiments show that $Mn^{2+}$ behaves much like $Ca^{2+}$ in that $Mg^{2+}$ does not compete well with $Mn^{2+}$ for binding in the HhH metal sites, but $Na^+$ does (Table 1). This places $Mn^{2+}$ next to $Ca^{2+}$ in the overall order of HhH metal ion binding preference: $Mg^{2+} < Ca^{2+}, Mn^{2+} < Na^{+} < Ba^{2+}, K^{+}$. These results are in agreement with the observation that, despite the relatively high (up to 5 mM) metal ion concentrations in the soaking solutions, there was no evidence of strong metal ion binding in any of the previous metal ion−nucleotide-soaked crystals (Pelletier et al., 1996b) (see footnote 1), thus giving an early indication that $Na^+$ ions compete well for binding in the HhH metal sites with all of the potential metal ions mutagens tested, including $Mn^{2+}$.

In a crystallographic experiment, $K^+$ ions are difficult to distinguish from transition metal ions such at $Mn^{2+}$ because they possess a comparable number of electrons (18 and 23 electrons for $K^+$ and $Mn^{2+}$, respectively). For this reason $K^+{-}Mn^{2+}$ competitive binding experiments have not been carried out with pol $\beta$−DNA cocrystals. However, perhaps it is reasonable to assume, with results from $Na^+{-}K^+$ competitive binding experiments, that $K^+$ ions probably block the binding of potential metal ion mutagens to the HhH metal sites even better than $Na^+$ ions do. This brings into question just how much of an effect a mutagen such as $Mn^{2+}$ can have on DNA binding for pol $\beta$ in vivo, especially considering $K^+$ ions are available in the cell at concentrations of about 100 mM, whereas $Mn^{2+}$ is a trace element with free metal ion concentrations probably on the order of 1 nM (Versieck & Cornelis, 1989). Although it is evident that much more work will be required to elucidate the effect of $Mn^{2+}$ ions on pol $\beta$ in vivo, two points are worth noting with regard to the results of our experiments: (i) pol $\beta$ solutions studies that were carried out in a buffer containing 100 mM KCl showed that $Mn^{2+}$, at concentrations ranging as low as 0.5 mM, had a measurable effect on the DNA binding properties of pol $\beta$ (Wang et al., 1977; Wang & Korn, 1982). This suggests that even very weakly bound $Mn^{2+}$ ions might have a tremendous effect on DNA binding, and such an effect is probably not easily detected by crystallographic techniques, where a sizable fraction of the $10^{14}$ molecules in a crystal must bind the metal ion in question before it is even observed. (ii) Crystallographic studies show that, in the presence of 150 mM NaCl, $Mn^{2+}$ still binds relatively strongly to the catalytic site of pol $\beta$, as well as to the nucleotide substrate (Pelletier et al., 1996b). These results suggest that any mutagenic effect that $Mn^{2+}$ might have on pol $\beta$ in vivo would most likely be caused by a distortion in nucleotide binding or by a change in the catalytic step itself (Pelletier et al., 1996b) and not by a distortion in DNA binding.

*The Magnetic Ball Bearing Model versus the Magnetic Railing Model.* Although the two HhH motifs in pol $\beta$ are structurally similar and bind DNA the same way, they appear to perform vastly different functions (Pelletier et al., 1996a). The HhH motif in the 8-kDa domain recognizes the 5′-$PO_4$ end of a DNA gap (Prasad et al., 1994) and may be capable of removing a 5′-deoxyribose phosphate intermediate prior to the gap-filling step in base excision repair (BER) processes (Matsumoto & Kim, 1995; Pelletier et al., 1996a). In contrast, the HhH motif in the fingers subdomain helps to position the primer strand of the DNA substrate in the polymerase active site. It has been proposed that the metal ion bound in the HhH motif of the fingers subdomain, in particular, may act as a processivity factor by increasing the affinity that pol $\beta$ has for the DNA substrate (in a non-sequence-specific manner) while, at the same time, facilitating movement of pol $\beta$ along the DNA backbone, and two different models for how a metal ion might do this were presented (Pelletier et al., 1996a). In the “magnetic ball bearing” model, the metal ion, which we now believe to be a $K^+$ ion in vivo, remains tightly bound to the carbonyl oxygens in the HhH binding pocket and, in effect, rolls in place as pol $\beta$ moves along the DNA. According to this model, metal ion coordinate bonds to DNA phosphate oxygen atoms are made and broken with each DNA translocation event. In contrast, in the “magnetic railing” model, metal ions are more closely associated with the negatively charged DNA phosphate oxygens than they are with the carbonyl oxygens of the HhH binding pocket, and pol $\beta$ glides along the DNA backbone on a metal ion track, or railing, that is formed by relatively tight associations between metal ions and DNA phosphates. According to this model, metal ion coordinate bonds are made and broken with the protein carbonyl oxygens, and a new metal ion enters the HhH binding pocket with each DNA translocation event. It should be noted that both of our processivity models assume that the translocation event, which is thought to be extremely rapid (Johnson, 1993), is faster than the rate of metal ion dissociation from the HhH metal site or from the DNA phosphate group when these two entities are separated from one another.

As described above, our failed attempt to back-soak $Na^+$ ions completely out of the HhH metal sites provides strong evidence that, in the presence of DNA substrate, the metal ion has a very slow rate of exchange with water molecules and remains tightly bound to the HhH metal pocket when a DNA phosphate ligand is provided (Figure 1). The favoring of one processivity model over another therefore depends on which group of oxygen ligands (the ones from the protein carbonyls or the ones from the DNA phosphates) have the greatest affinity for metal ions during the translocation event, when the HhH metal site and the DNA phosphate are briefly separated from one another. In an attempt to address this issue, crystal soaking experiments with 31-kDa apoenzyme crystals (no DNA bound) were carried out to determine if the HhH motifs have a high affinity for metal ions in the absence of DNA[2]. Results from these soaking experiments show that metal ions do not bind strongly to the HhH metal sites in the absence of DNA (Figure 1, middle and bottom panels; Table 1). Although these results appear to undermine the magnetic ball bearing model because all metal ions, including $K^+$, seem to have very little affinity for the free-standing cluster of carbonyl oxygen ligands in the HhH binding pocket, there is also no indication that metal ions, including $K^+$, bind strongly to the free-standing DNA phosphate groups in any of the crystal structures reported here nor in any of the previously reported crystal structures (Pelletier et al., 1996a,b)—a result that undermines the magnetic railing model. It is therefore not possible with the current crystallographic data to favor one model over another, and the dynamics of metal ion mediated processive polymerization for pol $\beta$ remains to be elucidated.

## ACKNOWLEDGMENT

We thank the personnel of the N. H. Xuong Laboratory for aid in data collection, especially C. Nielsen, N. Nguyen, and D. Sullivan, and we thank the personnel of the S. H. Wilson laboratory, especially W. Wolfle, for providing the human pol $\beta$ protein.

## REFERENCES

Cowan, J. A. (1993) *Inorganic Biochemistry, An Introduction*, VCH Publishers, New York.

da Silva, J. J. R. F., & Williams, R. J. P. (1991) *The Biological Chemistry of the Elements: The Inorganic Chemistry of Life*, Clarendon, Oxford, England.

Davies, J. F., Almassy, R. J., Hostomska, Z., Ferre, R. A., & Hostomsky, Z. (1994) *Cell 76*, 1123−1133.

Douglas, K. T., Bunni, M. A., & Baindur, S. R. (1990) *Int. J. Biochem. 22*, 429−438.

Evans, S. V. (1993) *J. Mol. Graphics 11*, 134−138.

Gale, E. F., et al. (1981) *The Molecular Basis of Antibiotic Action*, Chapt. 4, Wiley, New York.

Hamlin, R. (1985) *Methods Enzymol. 114*, 416−452.

Heaton, F. W. (1993) in *Magnesium and the Cell* (Birch, N. J., Ed.) Chapt. 8, Academic Press, San Diego, CA.

Howard, A. J., Nielsen, C., & Xuong, H. H. (1985) *Methods Enzymol. 114*, 452−472.

Johnson, K. A. (1993) *Annu. Rev. Biochem. 62*,

Kornberg, A., & Baker, T. A. (1992) *DNA Replication*, 2nd ed., Freeman, San Francisco, CA.

Kraulis, P. J. (1991) *J. Appl. Crystallogr. 24*, 946−950.

Lide, D. R. (1992) *CRC Handbook of Chemistry and Physics*, 73rd ed., CRC Press, Boca Raton, FL.

Matsumoto, Y., & Kim, K., (1995) *Science 269*, 699−702.

Moews, P. C., & Kretsinger, R. H. (1975) *J. Mol. Biol. 91*, 201−225.

Pelletier, H., Sawaya, M. R., Kumar, A., Wilson, S. H., & Kraut, J. (1994) *Science 264*, 1891−1903.
Pelletier, H., Sawaya, M. R., Wolfle, W., Wilson, S. H., & Kraut, J. (1996a) *Biochemistry 35*, 12742−12761.
Pelletier, H., Sawaya, M. R., Wolfle, W., Wilson, S. H., & Kraut, J. (1996b) *Biochemistry 35*, 12762−12777.
Prasad, R., Beard, W. A., & Wilson, S. H. (1994) *J. Biol. Chem. 269*, 18096−18101.
Sawaya, M. R., Pelletier, H., Kumar, A., Wilson, S. H., & Kraut, J. (1994) *Science 264*, 1930−1935.
Sirover, M. A., & Loeb, L. A. (1976) *Science 194*, 1434−1436.
Snow, E. T., & Xu, L. S. (1991) *Biochemistry 30*, 11238−11245.
Snow, E. T., Xu, L. S., & Kinney, P. L. (1993) *Chem.-Biol. Interact. 88*, 155−173.
Tronrud, D. E., Ten Eyck, L. F., & Matthews, B. W. (1987) *Acta. Crystallogr. A43*, 489−501.
Versieck, J., & Cornelis, R. (1989) *Trace Elements in Human Plasma or Serum*, CRC Press, Boca Raton, FL.
Wang, T. S.-F., Eichler, D. C., & Korn, D. (1977) *Biochemistry 16*, 4927−4934.
Wang, T. S.-F., & Korn, D. (1982) *Biochemistry 21*, 1597−1608.
White, S. P., Scott, D. L., Otwinowski, Z., Gelb, M. H., & Sigler, P. B. (1990) *Science 250*, 1560−1563.

BI960790I